

An SMDP Approach to Optimal PHY Configuration in Wireless Networks

Mark Shifrin, Daniel S. Menasché[§], Asaf Cohen, Omer Gurewitz, Dennis Goeckel*

Ben Gurion University of the Negev, [§]Federal Univ. of Rio de Janeiro, *Univ. of Massachusetts at Amherst

Abstract—In this work, we study the optimal configuration of the physical layer in wireless networks by means of Semi-Markov Decision Process (SMDP) modeling. In particular, assume the physical layer is characterized by a set of potential operating points, with each point corresponding to a rate and reliability pair; for example, these pairs might be obtained through a now-standard diversity-vs-multiplexing tradeoff characterization. Given the current network state (e.g., buffer occupancies), a Decision Maker (DM) needs to dynamically decide which operating point to use. The SMDP problem formulation allows us to choose from these pairs an optimal selection, which is expressed by a decision rule as a function of the number of awaiting packets in the source’s finite queue, channel state, size of the packet to be transmitted. We derive a general solution which covers various model configurations, including packet size distributions and varying channels. For the specific case of exponential transmission time, we analytically prove the optimal policy has a threshold structure. Numerical results validate this finding, as well as depict multi-threshold policies for time varying channels such as the Gilbert-Elliott channel.

I. INTRODUCTION

Recent advances in coding and modulation have allowed communication systems to approach the Shannon limit on a number of communication channels; that is, given the channel state (e.g. the signal-to-noise ratio of an additive white Gaussian noise - AWGN - channel), communication near the highest rate theoretically possible while maintaining low error probability is achievable. However, in many communication systems, particularly wireless communication systems, the channel conditions which a given transmission will experience are unknown. For example, consider the case of slow multipath fading without channel state information at the transmitter [1]. Because of the uncertainty in the level of multipath fading, it is possible that the rate employed at the transmitter cannot be supported by the channel conditions, hence resulting in packet loss or “outage”. The outage capacity [1], which gives the rate for various outage probabilities, captures the tradeoff in such a situation. If a low rate is employed, it is likely that the channel conditions will be such that transmission at that rate can be supported (low outage); if a higher rate is employed, the probability is higher that the channel conditions will be such that transmission at that rate cannot be supported (high outage). In fact, a wide range of physical layers models can be addressed through such an approach, i.e., having asymmetric characterization of the operating points and their corresponding parameters. Given this characterization, a crucial question is at which point to operate the physical layer given information available about the current state of the network.

Modern wireless networks are extremely dynamic, with channel parameters and traffic patterns changing frequently. Consequently, the key question addressed here is how can a sender *dynamically decide* on the best physical layer strategy, given the channel and traffic parameters available to it, as well as its own status. For example, consider a sender required to decide among the aforementioned physical layer strategies: an approach incurring high packet loss yet a small transmission time, or one possibly having a lower packet loss but a larger transmission time. In this paper, we derive a framework for a Decision Maker (DM) wishing to maximize the system throughput by choosing the appropriate physical layer setting, while taking into account as many system parameters as possible, in this case, delay, packet losses and its current packet backlog status. The DM faces a choice of achieving increased success probability provided additional transmission time, and one would expect that this decision will be made with the queue status in mind, as a full queue causes new arrivals to be rejected, incurring potential throughput loss. Thus, our goal is to rigorously analyze this tension, and identify the optimal strategy.

The tradeoff between rate and reliability is a fundamental characteristic of the physical layer, and we are interested in this formulation largely because it captures much more than the simple point-to-point single-antenna communication used for illustration in the first paragraph above. To provide a systematic method to consider how this characterization might be derived, consider the the now-standard diversity-multiplexing tradeoff approach originally applied to point-to-point multi-antenna systems [2] but now extensively extended beyond that. In particular, the diversity-multiplexing approach captures the fundamental tradeoff between rate (multiplexing) and reliability (diversity) for a number of interesting physical layer choices, including: (1) point-to-point multiple-input and/or multiple-output (MIMO) systems [2], where the transmitter can decide whether to send multiple streams (“multiplex”) from the multiple antennas or to send a single stream with redundancy (“diversity”), or a combination of the two; (2) half-duplex relay channels (e.g. [3]), where the transmitter can decide to use the relay, or not, and how to allocate time to the transmit and receive functions of the half-duplex relay. We are particularly interested in this latter example, and we will adopt terminology from a classical problem in relaying [4] to help clarify the competing options in succeeding sections. However, we hasten to remind the reader that the results apply much more generally to the diversity-multiplexing protocol for any physical layer.

A. Main contribution.

Our main contributions are as follows.

Problem formulation: We formulate the problem of optimal dynamic PHY configuration for the transmitter with long-lived packets influx by a SMDP. The model is presented in generality, capturing finite buffer size, variable packet size, variable channel state, general transmission time distribution and a decision space which is associated with possible PHY configuration.

Value function derivation: We derive the equations for the value function of the SMDP in several interesting cases. These equations are obtained in a tractable form, allowing a solution by simple value iteration.

Threshold policy characterization: When transmission times are exponentially distributed, we prove there exists an *optimal policy with a threshold structure*; that is, the source should make use of the more reliable option if the number of pending packets is lower than a given threshold, and transmit with the higher rate option otherwise. We also show that the value function in this case is concave and increasing.

Numerical study: We explore different scenarios by simulations. In particular, we validate the threshold policy and concavity for the exponential case and observe similarity to this structure in other cases as well. In the case of a variable channel (e.g., the Gilbert-Elliott channel) we observe a *multi-threshold* policy which is described by having a separate threshold for each channel mode.

To the best of our knowledge, this work is the first to *analyze* this problem of general optimal PHY operating point selection by SMDP.

B. Related work

The general trade-off between PHY rate and reliability has various important applications apart from the already mentioned basic relay channel. For example, the trade-off between multiplexing and diversity was discussed in [5] in the context of MIMO channels, in [6] in the context of multiple-access channel with fading, and in [7] in the context of cognitive radio sensing techniques. The SMDP framework introduced in this paper accounts for both space and time diversity.

Various PHY settings naturally reflect the diversity associated with wireless channel. Berry and Gallager [8] and Collins and Cruz [9] accounted for time diversity and delay constraints, while works such as Scaglione, Goeckel and Laneman [10] accounted for space diversity.

Routing solutions in wireless networks by means of queue stabilizations were first addressed in [11], and more recently in [12], [13]. Yeh and Berry in [12] considered control policies for cooperative relay selection. In particular, they used maximum differential backlog (MDB) methods to stabilize queues and to achieve the optimal throughput. The authors mainly concentrated on the transport level, hence did not capture physical level considerations e.g., fading environment. Our approach is different, as we combine the control on the packet (i.e. transport) level with PHY considerations, accounting for fading factors. In addition, note that we assume control of a *finite* queue, hence inherently stable. Recently, Urgaonkar and Neely [14] considered a constrained resource

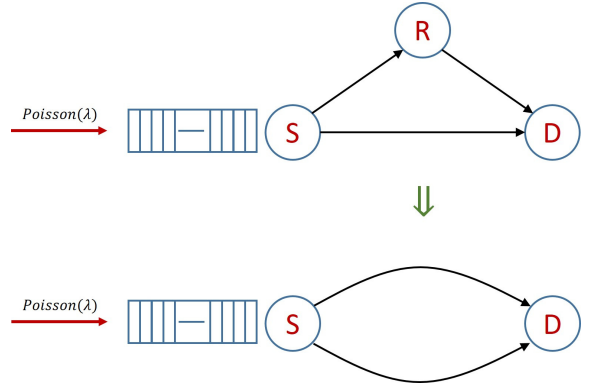


Fig. 1. Relay channel logical model

allocation problem in a relay network under stringent delay constraints.

[13] proposes near-optimal throughput proposing algorithms for finite queues. We consider a different approach to model the problem, namely a semi-Markov decision process (SMDP), which allows us to analyze a broader set of both PHY and transport level settings and channels, to provide an optimal policy, for which we prove structural properties.

The reliability versus delay trade-off in finite buffered wireless networks, accounting for multiple controllers, was considered in [15]. In a game-theoretic setting, players are coupled through their rewards, and act according to their local buffer and channel states, without being aware of the states and actions taken by other players.

For a basic introduction to SMDPs we refer the reader to [16]. A number of previous works on SMDPs have focused on establishing the existence of optimal policies of threshold type under a variety of settings [17], [18], [19], [20]. To the best of our knowledge, none of these works have addressed threshold properties for PHY operating points.

II. SYSTEM MODEL AND METRICS

The system is defined according to the following set of assumptions.

1) **Arrival process:** We assume that the data at the source is generated according to a Poisson process with intensity λ . In the case the source is busy with an ongoing transmission, the packets are fed into the *finite sized buffer*. The size of the buffer is known to the DM and is given by B packets slots. The packet sizes can vary, yet, for the model simplicity, it is assumed packets of all sizes occupy space of exactly one slot. Such a model can describe a setup in which the packets' descriptors are stored in the buffer whereas the varied size packets themselves are stored elsewhere. An extension which considers packets with varying buffer occupancy and specifically ones which occupy a varying number of *chunks* in the buffer is addressed in III-7. Packets arriving at a full buffer are rejected and the retransmission details are taken care of by higher layers.

2) **Operating points:** The source attempts to communicate the packet at the head of the queue to the destination by a choice among the possible *operating points* of the physical layer. For presentation and analytical simplicity, we assume at most two possible operating points at all decision epochs.

To exemplify this particular scenario, consider a simple half-duplex relay channel. In this case, we are motivated by the application of the diversity-multiplexing tradeoff to a classic half-duplex relay channel choice: the more reliable and lower relaying rate and outage probability from a prototypical early cooperative diversity protocol, and the less reliable and higher rate corresponding to the direct choice. While this choice applies cleanly to this simple example, the extension to the situation of more than two possible operating points, as might be appropriate for other PHY layer architectures, is straightforward. Henceforth, in all scenarios mentioned in this paper, a nomenclature of half-duplex relay channel will be used. We will always denote the more reliable path with a lower rate as path “a”, while the less reliable path with a higher rate will be denoted as path “b”. Denote the rates R_a and R_b , where $R_a < R_b$. The corresponding packet loss probabilities are denoted as p_a and p_b , where $p_a < p_b$ at all times. The reader should note that the limitation to only two operating points rules out the option of abstaining from a transmission. While the latter case opens an additional interesting tradeoff in certain cases (e.g., [15], [21]), we omit it here for the sake of simplicity of presentation. Yet, the straightforward extension to include the option of not to transmit for the certain time period is technically tractable; the interested reader is referred to the on-line version of the paper for the details.

3) **Transmission times:** The rates associated with the two operating points yield transmission time probability density functions (pdf) $g^a(t)$ and $g^b(t)$, which are readily calculated from R_a and R_b and, possibly, from other system parameters relevant at time t , as it is further specified in II-5 and II-4. Note that in the case of a half duplex relay model $g^a(t)$, refers to the entire path associated with choice “a”, even if the latter is subdivided into two separate paths. Therefore, the example of a half duplex relay obtains a simplified configuration, as Figure 1 demonstrates. See that the upper illustration particularly fits the relay channel problem, while the lower one can also refer to the general tension between two PHY settings associated with two different propagation paths; the upper path corresponds to the choice of reliability (diversity) while the lower path corresponds to the choice of rate (multiplexing).

4) **Packet size impact:** The transmission time is allowed to depend on the actual packet size. We consider *two modes* to capture such a dependency. In the first mode, the packet size cannot be timely sampled by the DM, hence is unknown prior to the transmission. Then, transmission times are random according to what is specified in II-3. In the second mode, the size can be sampled prior to the transmission. Then, the size of the packet to be transmitted is a part of the *state* and has impact on the decision. Denote the size of a packet in this case by k . Then, *packet size transition probabilities*, denoted by $q(k'|k)$, stand for the probability of having packet of size k' at the head of the queue after transmitting packet of size k . To this end, we assume a finite set of possible packet sizes such that $\sum_{k'} q(k'|k) = 1$. action u . The packet sizes can be coupled with transmission time distribution, hence, the corresponding pdf are given. We denote them by $g_k^a(t)$ and $g_k^b(t)$, and in the second mode they can be naturally assumed to be deterministic. In the detailed example presented in III-B

and in numerical study of this paper, we assumed the same packet loss probability for all packet sizes. However, once the size of the packet to be transmitted is a part of the state, the coupling of the packet size with the packet loss (e.g. by accounting for the BER) is straightforward and is transparently incorporated in our model. Note that q can capture complex packet arrival patterns. For example, a sequence of big packets which is likely to be followed by sequence of small packets and vice versa can be modeled provided the appropriate values for q are selected.

5) **Channel states and dynamics:** We consider a finite set of possible channel states, each state corresponding to a couple $h = (h_a, h_b)$. We assume that channel state dynamics can be modeled by a Markov process; that is, the *current channel statistics* are independent of the past given the last state of the channel. These dynamics reflect well-known channel models (e.g., i.i.d. fading, Gilbert-Elliott model. We provide a detailed example in III-C). The channel transition probability from state h to state h' is denoted by $p(h'|h)$. Clearly, $\sum_{h'} p(h'|h) = 1$. Next, consider a sequence of fading values observed across source packets, each value corresponding to a channel (or, separately, to each path) state. We assume that the statistics are known to the DM and are constant for a period which is significantly longer than the longest possible packet transmission time. The DM can obtain the packet loss probabilities associated with each such fading value for each potential PHY configuration. While these assumptions are approximations, they conform to the well-known realistic slow fading model, or quasi-static channels. Similarly to the impact of a packet size, the channel states can be coupled with transmission time distribution, hence, the corresponding pdf are given. We denote them by $g_h^a(t)$ and $g_h^b(t)$, and, in the general case, by $g_{h,k}^a(t)$ and $g_{h,k}^b(t)$. Clearly, different channel states correspond to different packet loss probabilities. In the Gilbert-Elliott model, for example, these probabilities can be calculated from the BER.

The tension between the operating points is summarized as follows: a higher transmission rate choice uses less resources (time) but at a higher packet loss probability, whereas a lower transmission rate choice exploits more resources to obtain a lower packet loss probability.

6) **General performance criterion:** Consider an SMDP with discounted cost functional, characterized by the tuple $\{\mathbf{S}, \mathbf{A}, \mathbf{P}, r, \gamma\}$, where the components are as follows. The state space \mathbf{S} expresses the set of all possible combinations of buffer state, channel state, and leading packet size. The action space \mathbf{A} is a set of actions which fits exactly one action to one operating point. The reward r is positive when a transmission was successful. The discount factor γ is an appropriately selected positive constant.

A decision must be made before every transmission. Let $\{\sigma_m\}$, $m = 0, 1, \dots$, be a time series where σ_m is the instant at which the m -th reward is added. Let r_m be a random variable characterizing the m th reward. Then, $r_m > 0$ when σ_m corresponds to a completion of a successful transmission; otherwise, $r_m = 0$. Since the average discounted infinite cost depends on the initial system state, it is given by $J^\pi(s_0) = \mathbb{E} \sum_{m=0}^{\infty} r_m e^{-\gamma \sigma_m}$. Write the discounted cost as the sum of

the reward obtained at the initial state and average discounted residual throughput profit associated with future rewards.

$$\begin{aligned} J^\pi(s_0) &= \mathbb{E}r^\pi(s_0)e^{-\gamma\sigma_0} + \mathbb{E}\sum_{m=1}^{\infty} e^{-\gamma\sigma_m} r_m \\ &= \mathbb{E}r^\pi(s_0) + J_1^\pi(s_0) \end{aligned} \quad (1)$$

Thus, our goal is the following:

Find the *dynamic physical layer setting selection policy* π , which takes as input the current occupancy of the buffer and information (if any) on the current channel state and the packet size at the source's queue head, and provide as an output a decision on which transmission path to employ, such that $J^\pi(s_0)$ is maximized.

Note that the analysis that follows can be easily extended to account for an average cost criteria, defined by $J^A = \lim_{N \rightarrow \infty} \frac{1}{N} \mathbb{E} \sum_{m=1}^N r_m$ in the sense that both criteria possess *similar optimal policies*. The connection between discounted and average infinite reward criteria is understood via Blackwell optimality as it is demonstrated in e.g., [22].

Hence, we formulate the described problem by a discounted SMDP, which is formally explained in the next section.

variable	description
λ	arrival rate
B	buffer capacity (including the packet being transmitted)
s	SMDP state (buffer state, channel state, leading packet size)
$V(s)$	value function at state s , $V(s) = \max_{u \in \{a, b\}} \{V^u(s)\}$
$V^u(s)$	cost associated with decision u at state s , $u \in \{a, b\}$
$\beta_{u,s}$	discount associated with action u
k	number of frames per packet
$\tau_{u,s}$	mean time to transmit via channel u at state s
$\mu_{u,s}$	transmission rate of channel u , $\tau_{u,s} = 1/\mu_{u,s}$
p_u	packet loss probability, $u \in \{a, b\}$
$g^\pi(t)$	pdf of transmission time then using policy π
$P^u(j i, t)$	probability of $j - i$ arrivals after t time units, given a buffer initially filled with i packets and action u is taken
$p(h' h)$	channel transition probabilities
$q(k' k)$	packet size transition probabilities

TABLE I
SMDP NOTATION.

III. SMDP-BASED FORMULATION AND SOLUTION

We start with definition of the state-space. A state $s \in \mathbf{S}$ is expressed by the triplet $(n, h, k) \in \mathbb{R}^3$ where n , h and k stand, respectively, for 1) the number of packets present in the system (including the one being transmitted), 2) the medium (channels) state and 3) the size of the packet which is to be transmitted in the upcoming transmission.

Transmissions can take one of two possible paths (“a” or “b”). Correspondingly, the action space is given by $\mathbf{A} = \{a, b\}$, standing for transmission modes “a” and “b”. We assume that a transmission decision with corresponding parameters is performed at every decision epoch.

State transitions occur after 1) transmission completions and 2) arrivals to an empty system. Right after a state transition due to a transmission completion occurs, a decision which sets the transmission mode of the next packet to be transmitted is made. If the system is non empty, a new transmission is immediately started. Otherwise, it starts whenever an arrival occurs.

The probability of having j packets in the buffer after a transmission of a packet of size k , taking t time units, when

the buffer initially contained i packets, is denoted by $\varrho(j|i, t)$ and is governed by a Poisson distribution with mean λt . If $j < B + 1$ and $i > 0$ then $j = i - k + m$, where m is the number of arrivals during an interval of length t . Let r be the instantaneous gain at the end of a successful transmission. It is given by k , in case the reward is set according to packet sizes, or constant equal 1 if successfully transmitted packets of all sizes have the same value.

Next, we expand the (1). Note that the second term of (1) is given by $\mathbb{E}_{(\sigma_1, s_1)}[e^{-\gamma\sigma_1} V(s_1)]$, where s_1 is the state following s_0 . The superscript π stands for the policy under consideration. Note that the value function V is obtained by maximizing J over all feasible policies, and is given by $V(s_0) = \max_{\pi} J^\pi(s_0)$, for all $s_0 \in \mathbf{S}$.

Denote the transition probability from state $s_0 = (i, h, k)$ to state $s_1 = (j, h', k')$ by $P(s_1|s_0, \pi(s_0), t)$. $P(s_1|s_0, \pi(s_0), t)$ depends on the arrival process, channel dynamics and leading packet size, and is given by

$$\begin{aligned} P(s_1|s_0, \pi(s_0), t) &= P((j, h', k')|(h, k, i), \pi(s_0), t) = \\ &= q(k'|k)p(h'|h)\varrho(j|i, t) \end{aligned} \quad (2)$$

where $\sum_{j, k', h'} q(k'|k)p(h'|h)\varrho(j|i, t) = 1$. The Bellman equation for the initial state s_0 , action $\pi(s_0)$ and next state s_1 is given by (1), setting $J_1^\pi(s_0)$ as follows

$$J_1^\pi(s_0) = \mathbb{E}e^{-\gamma t} \sum_{s_1} V(s_1)P(s_1|s_0, \pi(s_0) = u_0, t) \quad (3)$$

$$= \sum_{s_1} V(s_1) \int_0^\infty e^{-\gamma t} P(s_1|s_0, u_0) g^{u_0}(t) dt \quad (4)$$

$$= \sum_{h'} \sum_{k'} \sum_{j=i-k}^{B-k+1} V(s_1) \int_0^\infty e^{-\gamma t} P(s_1|s_0, u_0) g^{u_0}(t) dt. \quad (5)$$

The first (i.e the outer) summation in (5) is over all possible next channel states. It is degenerated if the channel state is fixed. The second summation is over all possible packet sizes to be transmitted at state s_1 . If the packet size is unknown at decision time, or all packet sizes are equal, this sum degenerates. The third summation is over the number of arrivals to the queue during a transmission. The integration accounts for the transmission time. Note that the transmission time pdf $g^{\pi(s_0)}$ may depend on the action taken in state s_0 . The expected instantaneous reward at state s_0 accounts for the average discount at the end of the transmission:

$$\mathbb{E}r^\pi(s_0) = \int r^{\pi(s_0)} e^{-\gamma t} g^{\pi(s_0)}(t) dt, \quad (6)$$

where $\pi(s_0) \in \{a, b\}$, $r^a = k(1 - p_a)$ and $r^b = k(1 - p_b)$.

The tractability of the Bellman equation form depends on resolvability of the integration in Equations (3)–(5). In the case a closed form can be obtained, a convenient utilization of value iteration (see, e.g., [16]) procedure is possible. In particular, Equations (3)–(5) substituted in (1) result in recursive equations. Then, the repetitious application of (1), guarantees an arbitrary closed convergence of V to the fixed point, which stands for the unique solution.

7) *Chunk granularity*: In order to consider packets, which can contain a variable number of chunks, several technical adjustments should be made. In particular, the Poisson *chunk arrival process* would feed the buffer room, which should be measured in *chunk units*. The packet size can be indicated within the last or the first chunk in a packet (i.e., in correspondence with the two modes of packet size impact on the decision making). The state definition should include the number of chunks in the buffer, hence, Equations (3)–(5) should be accordingly adjusted to reflect the change in the queue size after each transmission. In addition, the calculation of (6) should account for all additional states where the number of chunks present in the buffer is less than one packet.

A. Exponentially distributed transmission times

Let $1/\mu_u$ be the expected transmission time, $u \in \{a, b\}$.

1) *General SMDP formulation*: The state space is one-dimensional. Henceforth, we assume $B \geq 2$. The system state is characterized by the number of packets at the source, including the packet being transmitted, and is denoted by s , $s \in \{0, 1, \dots, B-1\}$. We assume all packets are equally valued with associated reward 1. Let $g^u(t) = \mu_u e^{-\mu_u t}$, where superscript u stands for the action taken, $u \in \{a, b\}$. Then, it follows from (4) that

$$J_1^u(j) = V(B-1) \int_0^\infty e^{-\gamma \tau_u} \rho(B|j, \tau_u) \mu_u e^{-\mu_u \tau_u} d\tau_u + \sum_{i=j-1}^{B-1} V(i) \left(\int_0^\infty e^{-\gamma \tau_u} \frac{e^{-\lambda \tau_u} (\lambda \tau_u)^{i-j+1}}{(i-j+1)!} \mu_u e^{-\mu_u \tau_u} d\tau_u \right)$$

where $\rho(B|j, \tau_u) = \left(1 - \sum_{i=j-1}^{B-1} \frac{e^{-\lambda \tau_u} (\lambda \tau_u)^{i-j+1}}{(i-j+1)!}\right)$ denotes the probability that during a transmission at least one packet is discarded due to buffer overflow, given that there are j packets in the system prior to the beginning of the transmission. Note that $\int_0^\infty t^n e^{-st} dt = \frac{n!}{s^{n+1}}$. Thus, for $0 < j \leq B-1$ we have,

$$J^u(j) = c_u \frac{\mu_u}{\mu_u + \gamma} + \sum_{i=j-1}^{B-1} V(i) \frac{\lambda^{i-j+1} \mu_u}{(\gamma + \mu_u + \lambda)^{i-j+2}} + V(B-1) \left(\frac{\mu_u}{\gamma + \mu_u} - \sum_{i=j-1}^{B-1} \frac{\lambda^{i-j+1} \mu_u}{(\gamma + \mu_u + \lambda)^{i-j+2}} \right), \quad (7)$$

where $c_u = (1 - p_u)$. The optimal value function is found by $V(n) = \max_u J^u(n)$, $n = 1, \dots, B-1$. Note that the value function at the boundary condition $n = B-1$ is obtained directly from the equations above, whereas $V(0)$ is given by

$$V(0) = \int_0^\infty e^{-\gamma t} \lambda e^{-\lambda t} V(1) dt = \frac{\lambda}{\lambda + \gamma} V(1). \quad (8)$$

Observe that (7) displays a quasi-closed form of the value function. This allows for convenient utilization of value iteration algorithm. In particular, by repetitious application of the recursive equations (7)–(8), V converges to the solution. Nevertheless, due to the summation in (7) the value function of the SMDP at each state may depend on all other states. For this reason, a direct analysis of V obtained from the SMDP formulation is cumbersome. To circumvent this challenge, we rely on an alternative MDP formulation which is equivalent to the SMDP presented above. The resulting Bellman equations

are simple, hence analysis and identification of optimal policies of threshold type is plausible.

2) *MDP formulation for the exponential case*: Next, we define the states of the MDP and their corresponding value functions. The transition diagram of the MDP is illustrated in Figure 2. The definition of the state space is inspired by the MDP admission control example presented in [16, chpt. 11].

Our goal is to leverage the Markovian structure of the problem when the times between all events are exponentially distributed. To this aim, we modify the state space to $\{0, 1, \dots, B-1\} \cup \{0, 1, \dots, B-1\} \times \{a, b\}$. In particular, we now consider transitions that occur *after every departure or arrival*. States (n) , $n = 0, \dots, B-1$, are achieved after a departure (transmission completion), whereas states (n, u) , $n = 0, \dots, B-1$, $u \in \{a, b\}$ are achieved after arrivals.

The system transitions to state (n) after a transmission completion that leaves behind n packets in the buffer. As soon as the system reaches state (n) , $n = 1, \dots, B-1$, the DM decides between transmitting the head-of-line packet through channels a or b . The mean residence time at state (n) , $n = 1, \dots, B-1$ is $1/(\mu_a + \lambda)$ or $1/(\mu_b + \lambda)$, if actions a or b are chosen, respectively. If a new packet arrives and encounters an idle system, the system transitions from state (0) either to state $(0, a)$ or $(0, b)$, depending on whether action a or b is chosen. The mean residence time at state (0) is $1/\lambda$.

Next, we consider a new packet that arrives to encounter a busy system. Immediately after the arrival the system transitions to state (n', u) , which accounts for the packet being transmitted, and where $n' = \min(B-1, n)$. At state (n', u) the DM does not take any actions, as the only possibility is to continue the ongoing transmission. The mean residence time at state (n', u) is $1/(\mu_u + \lambda)$.

Let $\mathcal{P}(s'|s, u)$ be the transition probability from state s to state s' , given that action u was taken. Then, for $n = 1, \dots, B-1$, the $\mathcal{P}(s'|s, u)$ is captured as follows.

$$\mathcal{P}(s'|s, u) = \begin{cases} 1, & s = (0), s' = (0, u) & (9a) \\ \frac{\lambda}{\lambda + \mu_v}, & s = (n), s' = (n, v), v = u \text{ or} & (9b) \\ \frac{\lambda}{\lambda + \mu_v}, & s = (n-1, v), s' = (n, v) & (9c) \\ \frac{\mu_v}{\lambda + \mu_v}, & s = (n), s' = (n-1), v = u \text{ or} & (9d) \\ \frac{\mu_v}{\lambda + \mu_v}, & s = (n, v), s' = (n) \text{ or} & (9e) \\ \frac{\mu_v}{\lambda + \mu_v}, & s = (0, v), s' = (0) & (9f) \end{cases}$$

A decision must be made when the system transitions to state (n) , $n = 0, \dots, B-1$. Note that decision u taken at state $s = (n)$ immediately impacts the upcoming system state through transitions (9a), (9b) and (9d). Transition (9a) occurs after an arrival to an empty system, whereas transitions (9b) and (9c) occur after arrivals to a busy system. Transition (9b) occurs after an arrival preceded by a transmission completion, when decision u had been made. Transition (9c) occurs after an arrival preceded by another arrival, during a transmission through channel v . Transitions (9d), (9e) and (9f) correspond to transmission completions. Transition (9d) occurs after a transmission completion which was preceded by another

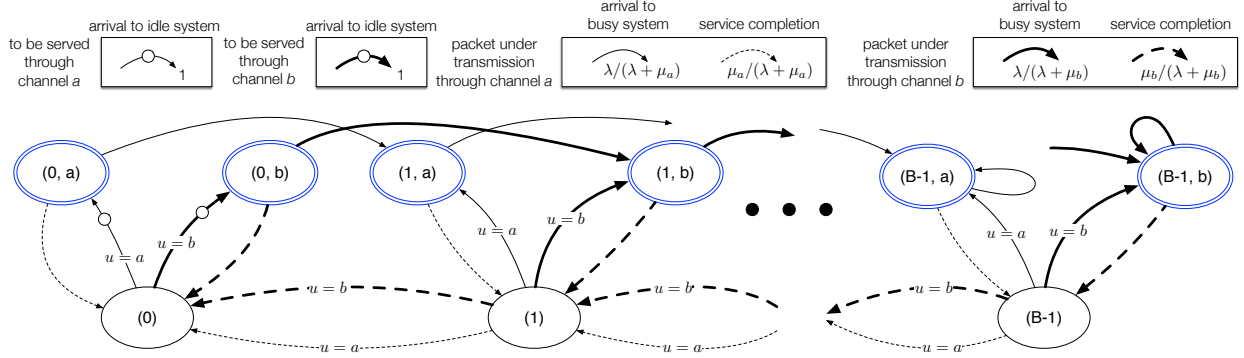


Fig. 2. MDP model of a system with buffer capacity B . Expected instantaneous reward c_a (resp., c_b) is received when action a (resp., b) is taken.

transmission completion, when decision u had been made. Finally, transitions (9e) and (9f) occur after transmission completions preceded by an arrival to a busy (resp., empty) system. Note that at states (n, a) and (n, b) the variable n does not account for the arriving packet, which will be admitted to the system in case the buffer is not full.

Instantaneous rewards are accumulated once transmissions are finished. Equivalently, such rewards are added at the beginning of a transmission, multiplied by the corresponding expected discount. In what follows, we let c_a and c_b be the expected instantaneous reward received when actions a and b are taken, respectively.

Next, we introduce the value functions and Bellman equations which characterize the solution of the MDP model. Recall that state (n, u) is achieved right *after* a departure (transmission completion) which leaves n packets at the buffer, $n \in \{0, 1, 2, \dots, B-1\}$. The value function for state (n) is denoted by V_n . Recall also that state (n, u) is achieved right *after* an arrival to a system with n packets, $n \in \{0, 1, 2, \dots, B-1\}$, including the one which is currently being transmitted on path u , $u \in \{a, b\}$. If $n = 0$, the transmission of the arriving packet is immediately started through u . The value function corresponding to state (n, u) is denoted by $V_n^{u,A}$ (“A” stands for “arrival”).

We are mainly interested in the values of states (n) , i.e., our main goal is to obtain V_n , $n \in \{0, 1, 2, \dots, B-1\}$, because the decisions are only made in these states and because they are comparable with the SMDP values.

Let $\delta_a = (\mu_a + \lambda + \gamma)^{-1}$, $\delta_b = (\mu_b + \lambda + \gamma)^{-1}$, $\beta_b = (\mu_b + \gamma)^{-1}$, $\beta_a = (\mu_a + \gamma)^{-1}$ and $\bar{\delta} = (\gamma + \lambda)^{-1}$. In what follows it will always hold $u \in \{a, b\}$. The Bellman equations define the operators \mathbb{A}_a and \mathbb{A}_b , which act in the space of function from $\{0, \dots, B\}$ to \mathbb{R} . Write

$$V_n^{u,A} = \mu_u \delta_u V_n + \lambda \delta_u V_{n+1}^{u,A} = \mathbb{A}_u V_n^{u,A} \quad (10)$$

Denote by $\mathbb{T}, \mathbb{T}_a, \mathbb{T}_b$ the operators acting on the space of functions from $\{0, \dots, B\}$ to \mathbb{R} . When applied to state n , these operators yield the following equation for $u \in \{a, b\}$:

$$V_n^{u,D} = \mathbb{T}_u V_n = \mu_u \delta_u V_{n-1} + \lambda \delta_u V_n^{u,A} + (1 - p_u) \beta_u \quad (11)$$

The maximization over the available actions is performed after transmission completions, at states (n) , $n = 1, \dots, B-1$, when n packets are left in the buffer,

$$V_n = \max(V_n^{b,D}, V_n^{a,D}) = \mathbb{T} V_n = \max(\mathbb{T}_b V_n, \mathbb{T}_a V_n). \quad (12)$$

variable	description
c_u	expected instantaneous reward associated to decision u .
(n, u)	state right after arrival, when current active transmission is through u and n packets are found by the arrival.
(n)	state following a transmission completion, when n packets are left in the buffer. Decisions are made at these states.
$V_n^{u,A}$	value function at state (n, u) .
V_n	value function at state (n) , $V_n = \max\{V_n^{a,D}, V_n^{b,D}\}$.
$V_n^{u,D}$	state-action value function for action u at state (n) .
\mathbb{A}_u	operator applied over arrivals (acts on $V_n^{u,A}$).
\mathbb{T}_u	operator applied over departures (acts on $V_n^{u,D}$).
\mathbb{T}	operator that maximizes the outcome of \mathbb{T}_u over u .

TABLE II
MDP NOTATION ($u \in \{a, b\}$, $n \in \{0, \dots, B-1\}$).

At the buffer limit boundary B we have

$$V_B^{u,A} = \mu_u \delta_u V_{B-1} + \lambda \delta_u V_B^{u,A} \quad (13)$$

and at the empty buffer,

$$V_0^{b,D} = V_0^{a,D} = \max(\lambda \bar{\delta} V_0^{b,A}, \lambda \bar{\delta} V_0^{a,A}). \quad (14)$$

Arrivals that find an empty buffer are subject to the effect of the DM current decision,

$$V_0^{b,A} = V_0^{a,A} = \max_{u \in \{a, b\}} (\mu_u \delta_u V_0^{u,D} + \lambda \delta_u V_1^{u,A} + c_u) \quad (15)$$

Note that $V_0^{b,A} = V_0^{a,A}$ holds because at state (0) no packet is currently being transmitted. The derivation of equations (10)-(15) from the process model is presented in Appendix A.

In Section IV we will use the MDP formulation to identify the threshold type structure of the optimal policy.

B. Deterministic transmission times and known packet sizes

Consider a source which samples the packet size before the transmission. Consider two possible sizes, denoted by k_1 and k_2 , both taking in the buffer exactly one slot. We assume equal rewards for both sizes. Then, the state is given by $s = \{n, k\}$, $n \in \{0, \dots, B\}$ and $k \in \{k_1, k_2\}$. We assume that packet size dynamics is given by a discrete Markov Chain with transition probabilities $q(k'|k)$. Denote the deterministic transmission time of packet of size k as $\tau^\pi(n, k)$. The packet loss probabilities are p_a and p_b . Denote $s_0 = (i, k)$, $s_1 = (j, k')$. Then,

$$J_1^\pi(i, k) = \sum_{k'} \sum_{j=i-1}^B e^{-\gamma \tau^\pi(s_0)} Q((s_1)|s_0, \pi(s_0)) V(j, k')$$

where $Q((s_1)|s_0, \pi(s_0)) = q(k', k)\varrho(j|i, \tau^{\pi(s_0)})$. See that $c_{\pi(i,k)} = \mathbb{E}r^{\pi(i,k)} = (1 - p_{\pi(i,k)})e^{-\gamma\tau^{\pi(i,k)}}$. Hence, the value functions are $V(i, k_m) = \max_{\pi}\{J^{\pi(i,k_m)}\}$, $m \in \{1, 2\}$. Finally, the boundary condition, then the buffer is empty is

$$V(0, k) = \mathbb{E}e^{-\gamma t} V(1, k) = \sum_{k'} \frac{\lambda}{\gamma + \lambda} (q(k'|k, 0)V(1, k')).$$

C. Gilbert-Elliott channel, uniformly distributed transmission times

Assume the packet sizes cannot be sampled, but are known to have a uniform distribution over all channels. Consider a Gilbert-Elliott (G-E) channel with two states, Good and Bad, denoted by \mathcal{G} and \mathcal{B} . For simplicity, we assumed a similar state for the entire medium, that is $h \in \{h^{\mathcal{G}}, h^{\mathcal{B}}\}$, such that $h^{\mathcal{G}} = (h_a^{\mathcal{G}}, h_b^{\mathcal{G}})$, $h^{\mathcal{B}} = (h_a^{\mathcal{B}}, h_b^{\mathcal{B}})$, where a, b stand for the two operating points, i.e., channel ‘‘a’’ (e.g., the relay channel) and channel ‘‘b’’ (e.g., the direct channel). We assume that channel dynamics can be expressed by discrete Markov Chains. The channel state is sampled prior to each upcoming transmission, and is modeled as part of the state space. Hence, the state is given by $s = \{n, h\}$, $n \in \{0, \dots, B\}$ and $h \in \{\mathcal{G}, \mathcal{B}\}$. The packet loss probabilities can be calculated right before the current transmission slot. According to the number of possible channel states, there are two possible packet loss probability ordered pairs: $(p_a^{\mathcal{G}}, p_b^{\mathcal{G}})$ and $(p_a^{\mathcal{B}}, p_b^{\mathcal{B}})$. We assume these probabilities are calculated from the BER which corresponds to the particular G-E channel state. Denote $u = \pi(n, h)$. The transmission time $\tau^{a,h}$ (resp. $\tau^{b,h}$) over channel ‘‘a’’ (resp. channel ‘‘b’’) is uniformly distributed. The uniform distributions intervals are given by $[\alpha_{h_u}, \beta_{h_u}]$. The channel transition probabilities, are denoted by $p(h'|h)$. Notation is summarized in Figure 3.

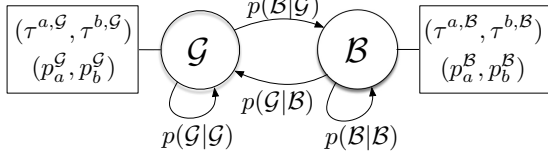


Fig. 3. Gilbert-Elliott model

Denote $s_0 = (i, h)$, $s_1 = (j, h')$, $h, h' \in \{\mathcal{G}, \mathcal{B}\}$. Then,

$$J_1^u(s_0) = \sum_{j=i-1}^B \sum_{h'} V(j, h') \int_{\alpha_{h_u}}^{\beta_{h_u}} e^{-\gamma t} Q(s_1|s_0, \pi(s_0)) dt$$

where $Q(s_1|s_0, \pi(s_0)) = (\beta_{h_u} - \alpha_{h_u})^{-1} \varrho(j|i, t)p(h'|h)$, and $(\beta_h - \alpha_{h_u})\mathbb{E}r^u = (1 - p_u) \int_{\alpha_{h_u}}^{\beta_{h_u}} e^{-\gamma t} dt = (1 - p_u)e^{-\gamma(\beta_{h_u} - \alpha_{h_u})}$. Note that the probability to have full buffer after end of transmission is given by $\varrho(B|i, t) = (1 - \sum_{i=j-1}^{B-1} \varrho(j|i, t))$. Finally, the value function for state s is given $V(s) = \max_u \{J^u(s)\}$.

IV. STRUCTURE OF OPTIMAL POLICIES

The structure of the optimal policy has a particular importance, in the sense that it can facilitate assessment of resources needed for the policy implementation at wireless nodes. For the system with large state-space, structural properties can be

exploited by learning algorithms in order to significantly reduce the complexity of optimal policy search. For example, once the policy is proven to possess a *threshold* structure, the data to hold for the policy (in the corresponding dimension of a state space) is reduced to a single scalar. Moreover, the configuration of similar systems can be analytically or heuristically based on the existing one, e.g. by means of reinforcement learning aimed to policy improvement. We aim to identify threshold policies for the SMDP models and solutions presented above. For the exponential case, we analytically prove the threshold property. We finally compare by simulations the thresholds associated with other transmission time distributions. To this end, we state our main analytical result:

Theorem 1. *The problem with exponentially distributed transmission times modeled by MDP is solved by the optimal policy of a threshold type. Namely, there exists a unique threshold t , $0 \leq t \leq B$, such that the optimal policy is to transmit via path ‘‘a’’ for all states where $n \leq t$ and to transmit via path ‘‘b’’ otherwise.*

By the equivalence of the value functions at departures in MDP and SMDP formulations trivially the following holds.

Corollary 1. *The exponential problem modeled in section III by SMDP is solved by the optimal policy of threshold type.*

To this end, let \mathcal{S} be a set where each of its elements is a five-tuple of B -dimensional vectors denoted by $\{U, U^{b,A}, U^{a,A}, U^{b,D}, U^{a,D}\}$ satisfying the following properties

- 1) the difference $U_n^{a,D} - U_n^{b,D}$ is non-decreasing in n , $n \in \{0, \dots, B\}$
- 2) $\{U^{b,D}, U^{a,D}, U^{b,A}, U^{a,A}\}$ are concave in $n \in \{1, \dots, B\}$,
- 3) $\{U, U^{b,A}, U^{a,A}\}$ are non-decreasing in $n \in \{0, \dots, B\}$,
- 4) $\{U, U^{b,A}, U^{a,A}\}$ have their slope bounded by some positive constant K , that is, $U_n - U_{n-1} < K$, $U_n^{a,A} - U_{n-1}^{a,A} < K$ and $U_n^{b,A} - U_{n-1}^{b,A} < K$. For the proof of the theorem we will need the following lemma.

Lemma 1. *The operators $\mathbb{A}_b, \mathbb{A}_a, \mathbb{T}$ preserve properties 1)-4).*

The proof of the lemma appears in Appendix B.

Proof of Theorem 1. We rely on a well known result that operators associated with Bellman equation are contracting [16], that is, using the maximum metric $\|U\| = \max_x |U(x)|$ it holds $a \|U - W\| < \|TU - TW\|$ for some $0 < a < 1$. Hence, the operators defined above are contraction mappings, equipped with the metric $\rho(U; W) = \|U - W\|$ in a complete metric space. Since \mathcal{S} is a complete metric space and the operators are strict contractions, they have corresponding fixed points (e.g. [23, Theorem V.18]). Now since \mathcal{S} is not empty (one can easily construct such functions; the technical details are omitted), the functions which are in \mathcal{S} and have the operators $\mathbb{A}_a, \mathbb{A}_b, \mathbb{T}$ applied on them, by lemma 1 stay in \mathcal{S} . By contraction, the repetitious application brings the result infinitesimally close to the fixed points of $\mathbb{A}_a, \mathbb{A}_b, \mathbb{T}$. Recall that the value functions $V_n, V_n^{b,A}, V_n^{a,A}$ are the unique solution of *all* functions, including those that in \mathcal{S} , acting from $n \in \{0, \dots, B\}$ to \mathbb{R} , to the *same* equations; (trivially, the mild

conditions for uniqueness and existence, see e.g. [16, Chapter 6.2], apply). As a result, $\{V, V^{b,A}, V^{a,A}, V^{b,D}, V^{a,D}\}$ coincide with these fixed points and they are in \mathcal{S} . In particular, $V^{b,D}$ and $V^{a,D}$ possess property 4), which is equivalent of having at most one policy switch state. This proves the proposition. \square

V. NUMERICAL RESULTS

In this section, we report numerical results on the shape of the value functions obtained through value iteration. Our goals are to 1) illustrate how different system parameters impact the performance of threshold policies and 2) numerically investigate the optimality of multi-threshold optimal policies for the Gilbert-Elliott channel.

The parameters chosen in the numerical experiments that follow in this section were selected for illustrative purposes, and are set according to the experimental goals.

A. Value functions

In Figure 4, we compare the value functions and threshold policies for channels associated with exponential, deterministic and uniform transmission times. The mean transmission rates were set to $\mu_a = 9$ and $\mu_b = 12$, under channels a and b , respectively. The support of the uniformly distributed transmission times was set to $[\alpha, \beta]$, where $\alpha = 0.2/\mu_u, \beta = 1.8/\mu_u$ and $u \in \{a, b\}$. We considered both a low load ($\lambda = \mu_a = 9$) and a high load ($\lambda = \mu_b = 12$) regime. Vertical lines show the thresholds where the policy determines a switch from a to b .

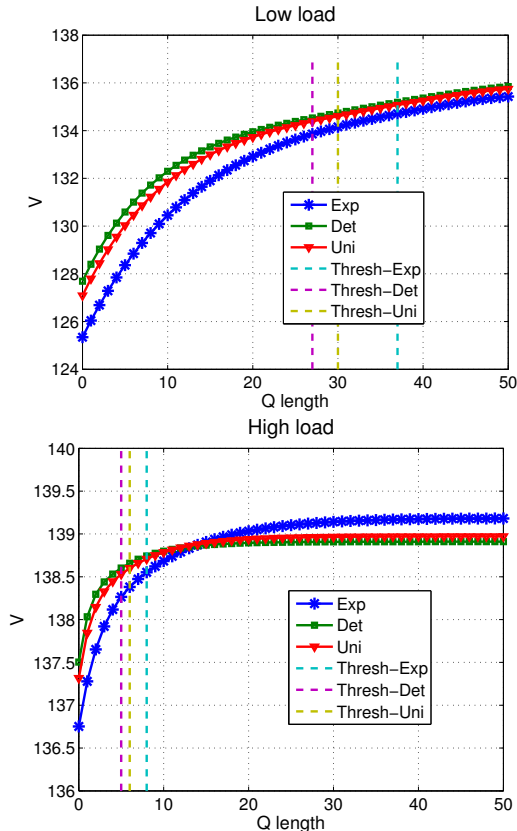


Fig. 4. Value functions, $V(\cdot)$, at different buffer states, n , when channel states are sampled from an i.i.d. model. Average transmission rates and packet losses are given by $\mu_a = 9, p_{a,A} = 0.25$ and $\mu_b = 12, p_{b,B} = 0.42$, under high load ($\lambda = 13$) and low load ($\lambda = 9$).

Observe that under high load the thresholds are significantly smaller than under low load. This is because in the latter case it is important to avoid buffer underflows, which cause a reduction in system throughput. For the high load, see that at the states close to B the value function becomes nearly constant. This may be explained by the fact that in all these states the average time until the buffer empties is large.

Also note that the numerical results validate our formal results on the concavity of the value function for the exponential case. In addition, the value function for the two other cases are observed to have a concave form, an observation which is interesting on its own.

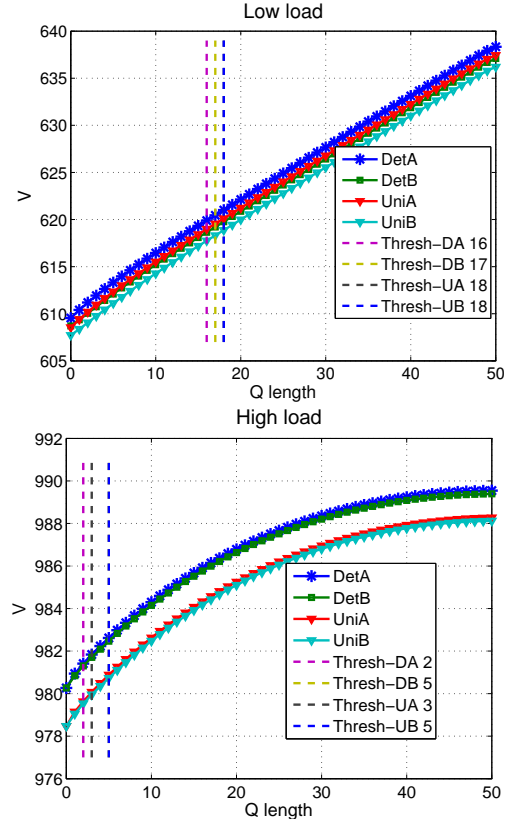


Fig. 5. Value functions, $V(\cdot)$, at different buffer states, n , when channel is characterized by a Gilbert-Elliott model. Parameters are given by $\mu_a = 10, p_{a,A} = 0.2, p_{a,B} = 0.35$ and $\mu_b = 15, p_{b,A} = 0.3, p_{b,B} = 0.4$, under high load ($\lambda = 15$) and low load ($\lambda = 10$). The optimal threshold values are marked using vertical lines.

Figure 5 illustrates the multi-threshold policies obtained when solving the SMDP model under deterministic and uniform transmission times with Gilbert-Elliott channels. The two channel states are denoted as \mathcal{A} and \mathcal{B} . Each transmission time distribution corresponds to *two* value functions, for channels at states \mathcal{A} and \mathcal{B} . Hence, each value function implies its own threshold. Observe that the value functions for \mathcal{A} and \mathcal{B} are very close to each other. Nonetheless, the thresholds can be easily distinguished. Under the Gilbert-Elliott channel model, for all the scenarios considered we were always able to find a separate threshold for each channel type. While a rigorous analysis of the multi-threshold policy is subject for a future work, the numerical analysis presented here can be used to devise heuristics to be concurrently applied with value iteration,

aiming towards a faster convergence.

B. Impact of thresholds

Next, we illustrate the impact of the thresholds on the throughput. Our goals are to assess, 1) for a given service distribution, how the throughput varies as a function of the threshold, and 2) how the service distribution impacts the optimal threshold. To this aim, we consider exponential, deterministic and uniform service distributions.

Policy evaluation was performed using three different techniques under the exponential, deterministic and uniform service time distributions. Under exponentially distributed service times, given a fixed threshold policy the resulting system dynamics is governed by a continuous-time Markov chain (CTMC). Impulse rewards are accumulated at service completions, and system throughput is given by the expected impulse reward of the resulting CTMC. For the deterministic case, we rely on a special class of solution methods to efficiently compute metrics of interest for models wherein all events are exponentially distributed except for a single deterministic one [24]. For uniform service times, we make use of [25]. The results for the exponential and deterministic service times were obtained using the Tangram II tool [26], whereas the uniform case was evaluated using the Oris tool [25]. More details are found in Appendix C.

In Figure 6 we let $B = 10$ and allow the threshold to vary between 0 and 9. We let $\lambda = 17$, $C = 1$, $p_b = 0.42$, $p_a = 0.25$, $\mu_b = 13$ and $\mu_a = 10$. Note that as the threshold increases the throughput first increases and then decreases. A threshold of 0 (resp., 9) consists of always transmitting through the less reliable channel, i.e., channel “b” (resp., through the most reliable channel, i.e., channel “a”). The optimal threshold equals 3, 4 and 6 for deterministic, uniform and exponential service distributions. As the variability in the service time increases, the optimal strategy privileges transmissions through the most reliable channel.

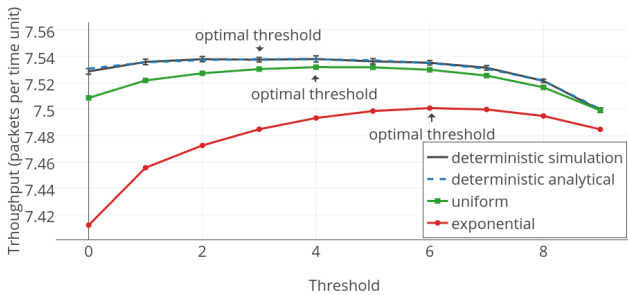


Fig. 6. Throughput as a function of threshold ($B = 10$). As the variability in the service time distribution increases, the optimal threshold increases.

Next, we let $B = 50$ and $\lambda = 13$, and keep the other parameters unchanged (Figure 7). Similar observations as made in the previous paragraph apply. In all the considered cases, there is a unique optimal threshold. The optimal threshold equals 12, 15 and 21 for deterministic, uniform and exponential service distributions (see Figure 8).

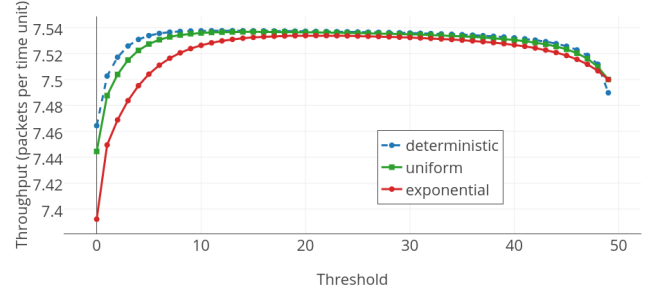


Fig. 7. Throughput as a function of threshold ($B = 50$). As the threshold increases, the throughput first increases and then decreases.

As a sanity check, we also ran simulations for deterministic service times, using the Tangram II tool [26]. For each set of parameters, we ran 30 simulation runs. Each run lasted for 100.000 time units. We confirmed that the results obtained through simulations and analytically are in conformance. The 95% confidence intervals in Figures 9 and 6, obtained through simulations, are in agreement with the analytical results, reported as dotted lines.

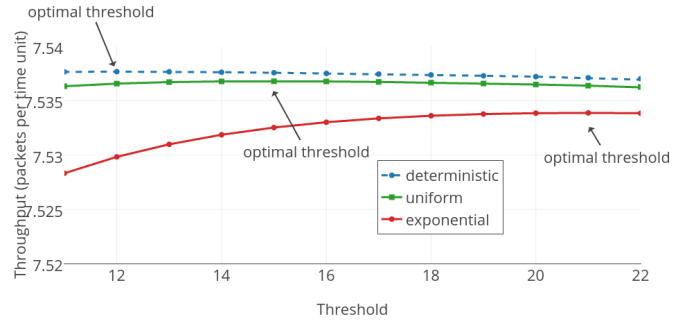


Fig. 8. Throughput as a function of threshold ($B = 50$) (zoom of Figure 7). As the variability in the service time distribution increases, the optimal threshold increases.

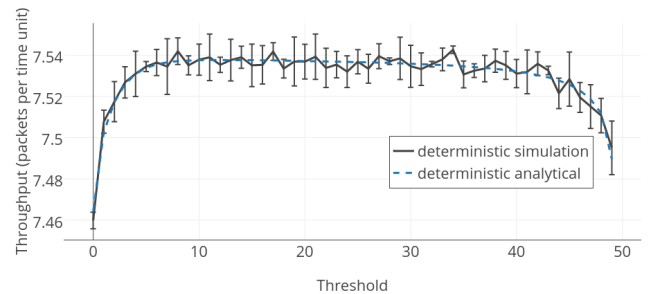


Fig. 9. Throughput as a function of threshold ($B = 50$). Results obtained analytically and through simulations are in agreement.

As indicated above, the numerical examples suggest that the optimal threshold increases with respect to the variability in the service time distribution. Verifying such a conjecture is subject for future work. Note also that in the illustrative results reported in this section the throughput values vary between 7.4 and 7.6. Although in the presented examples the range of

throughput values is short, in general it can be arbitrarily large, further motivating the search for the optimal threshold value.

VI. CONCLUSION

We have proposed an SMDP model for optimal PHY configuration, derived equations for the value function for several interesting cases, and formally shown structural properties of the optimal policy when transmission times are exponentially distributed. In particular, we have shown the existence of optimal policies of threshold type. The numerical solution of the proposed model indicates the existence of multi-threshold policies for Gilbert-Elliott channels. Showing the optimality of the latter under general settings is an interesting open problem.

APPENDIX

A. Bellman equation for the exponential case

Next, our goal is to derive the Bellman equations (10)-(15) from the process model. We consider exponentially distributed service times.

Denote by $u_n = 0$ the decision to send through channel “b” and $u_n = 1$ through channel “a”. We assume a stationary policy.

Note that the reward (c_a or c_b) is immediately received at $V_n(t)$. Take infinitesimal θ , such that probability that more than one event occur in $[0, \theta]$ goes to zero.

Use dynamic programming principle to write

$$V_n(t) = \int_t^{t+\theta} e^{-\gamma s} r(s) dR(s) + e^{-\gamma(\theta+t)} V_n(t+\theta), \quad (16)$$

where $r(s)$ denotes reward at time instant s , $R(s)$ is Poisson counting process which mean will be specified below. Due to the stationary property we will assume the initial time $t = 0$, and will omit the time mark where it is clear. To assume the immediate reward we take θ infinitesimal. Denote $\int_0^\theta e^{-\gamma s} r(s) dR(s) = r_\theta$.

Then, write

$$\begin{aligned} V_n &= r_\theta + \\ &+ e^{-\gamma\theta} \left[\theta\lambda(1-u_n)V_n^{b,A} + \theta\lambda u_n V_n^{a,A} \right. \\ &+ \theta\mu_a u_n V_{n-1} + \theta\mu_b(1-u_n)V_{n-1} + \\ &\left. V_n(1 - \theta\lambda(1-u_n) - \theta\lambda u_n - \theta\mu_a u_n - \theta\mu_b(1-u_n)) \right] \end{aligned}$$

The term in brackets sums up all possible outcomes for the value function at time θ weighted by the corresponding probabilities. (e.g. arrivals happen w.p. $\lambda\theta$). Now, since θ is small, substitute $e^{-\gamma\theta} \approx 1 - \gamma\theta$,

$$\begin{aligned} V_n &= r_\theta + (1 - \gamma\theta) [\theta\lambda(1-u_n)V_n^{b,A} + \theta\lambda u_n V_n^{a,A} + \\ &\theta\mu_a u_n V_{n-1} + \theta\mu_b(1-u_n)V_{n-1} + \\ &V_n(1 - \theta(1-u_n + u_n)\lambda - \theta\mu_a u_n - \theta\mu_b(1-u_n))] \end{aligned}$$

See that $\theta^2 \rightarrow 0$

$$\begin{aligned} V_n &= r_\theta + [\theta\lambda V_{n+1} + \\ &\theta\mu_a u_n V_{n-1} + \theta\mu_b(1-u_n)V_{n-1} + \\ &V_n(1 - \theta\lambda - \theta\mu_a u_n - \theta\mu_b(1-u_n)) - \gamma\theta V_n] \end{aligned}$$

Denote $\delta^{-1} = \lambda + \mu_b u + \mu_a(1-u_n) + \gamma$. See that V_n cancel on both sides.

$$\begin{aligned} 0 &= r_\theta + [\lambda(1-u_n)V_n^{b,A} + \lambda(u_n)V_n^{a,A} + \\ &\mu_a u_n V_{n-1} + \mu_b(1-u_n)V_{n-1} - \delta^{-1}V_n] \theta \end{aligned}$$

Calculate now r_θ . The reward is received in all possible cases. That is, whenever the process does not change, arrival happens or transmission ends. Hence, at V_n we have a reward approximately accumulated with Poisson process with mean rate $\lambda + \mu_a u_n + \mu_b(1-u_n) + \gamma$, where the terms stand for summation of the rates of arrival, transmission on path a , transmission on path b and the discounting rate. Hence, $dR = dt(\lambda + \mu_a u_n + \mu_b(1-u_n) + \gamma)$. Substitute

$$\begin{aligned} \int_0^\theta e^{-\gamma t} r(s) dR(s) &= \\ &= (\lambda + \mu_a u_n + \mu_b(1-u_n) + \gamma) C \int_0^\theta e^{-\gamma t} dt \\ &= (\lambda + \mu_a u_n + \mu_b(1-u_n) + \gamma) C \frac{1 - e^{-\gamma\theta}}{\gamma} \\ &= \theta(\lambda + \mu_a u_n + \mu_b(1-u_n) + \gamma) C \end{aligned}$$

where $r(s) = C$ for $s \in (0, \theta)$, while $C = (1-u_n)c_b + u_n c_a$. Note that

$$c_b = (1-p_b) \int_0^\infty e^{-\mu_b t} e^{-\gamma t} dt = (1-p_b) \frac{\mu_b}{\gamma + \mu_b}$$

c_b stands for average reward equal to $1 - p_b$, discounted according to the transmission time. c_a is equivalently calculated. Finally, substitute the reward

$$V_n \theta \delta^{-1} = \theta(\lambda + \mu_a u_n + \mu_b(1-u_n) + \gamma) C + \quad (17)$$

$$\begin{aligned} &[\lambda(1-u_n)V_n^{b,A} + \lambda(u_n)V_n^{a,A} + \\ &\mu_a u_n V_{n-1} + \mu_b(1-u_n)V_{n-1}] \theta + o^2(\theta) \quad (18) \end{aligned}$$

Since the routing decision is applied on u_n , the Bellman equation follows by the maximization over $u_n = \{0, 1\}$. Substitute the max operator, divide by $\theta\delta^{-1}$, and let $\theta \rightarrow 0$,

$$V_n = \max[c_a + \mu_a \delta_a V_{n-1} + \lambda \delta_a V_n^{a,A}, c_b + \mu_b \delta_b V_{n-1} + \lambda \delta_b V_n^{b,A}]$$

□

B. Proof of lemma 1

For simplicity we assume all packets are equally rewarded by $r = 1$. Denote $c_b = (1-p_b)\beta_b$ and $c_a = (1-p_a)\beta_a$.

Proof. To show that operators $\mathbb{A}_b, \mathbb{A}_a, \mathbb{T}$ preserve properties 1)-4) construct first some $\{U, U^{b,A}, U^{a,A}\}$, prior to applying the operators on them, such that $U^{b,A}, U^{a,A}$ and U are non-decreasing, concave and bounded. Moreover, the further construction of $U^{b,D}$ and $U^{a,D}$ using $\{U, U^{b,A}, U^{a,A}\}$ and applying (11) on them, is such that $U_n^{b,D} - U_n^{a,D}$ is non-decreasing in n . Note that by non-decreasing property of $U^{b,A}, U^{a,A}$ and U such a construction is straight-forward (we omit the detailed construction procedures). Also note that by concavity of $U_n^{b,A}, U_n^{a,A}$ and $U_n, U_n^{b,D}$ and $U_n^{a,D}$ are also concave in n , since they are positive linear sum of concave functions. Hence, $\{U, U^{b,A}, U^{a,A}, U^{b,D}, U^{a,D}\} \in \mathcal{S}$.

Denote $D_n = \mu_b \delta_b U_n + \lambda \delta_b U^{b,A}_{n+1} =$ and $R_n = \mu_a \delta_a U_n + \lambda \delta_a U^{a,A}_{n+1}$. By construction, $D_n = U_n^{b,D} - c_b$, $R_n = U_n^{a,D} - c_a$, hence, are concave. By property 1, $D_n - R_n$ is an increasing sequence.

At $n = 0$, $D_0 = U_0^{b,D}$, $R_0 = U_0^{a,D}$. By boundary condition (14), $D_0 = R_0$, hence it always holds $D_n > R_n$. To this end, define the slope of some discrete W_n , $n \in \{0 \cdots B - 1\}$ as $\Delta(W_n) = \Delta W_n = W_{n+1} - W_n$. Clearly,

$$\Delta(D_n) > \Delta(R_n) \quad (19)$$

By concavity $\Delta(D_n)$ and $\Delta(R_n)$ are decreasing sequences, hence $\Delta(D_n) + \Delta(R_n)$ is also decreasing. Next, write

$$\Delta(D_n) + \Delta(R_n) = (D_n - R_{n-1}) + (R_n - D_{n-1})$$

Clearly, at least one of the two sequences $D_n - R_{n-1}$ and $R_n - D_{n-1}$ is decreasing. Assume that, $D_n - R_{n-1}$ is increasing. However, then $\Delta(R_n - D_{n-1}) > \Delta(D_n - R_{n-1})$, hence $\Delta(R_n) + \Delta(R_{n-1}) > \Delta(D_n) + \Delta(D_{n-1})$, which contradicts (19), thus the assumption above is incorrect and the sequence $D_n - R_{n-1}$ is increasing in n .

We show next that applying the corresponding operators results in functions which possess these properties as well. Namely, $\{\mathbb{T}U, \mathbb{A}_b U^{b,A}, \mathbb{A}_a U^{a,A}, \mathbb{T}_b U^{b,D}, \mathbb{T}_a U^{a,D}\} \in \mathcal{S}$. Note that the preservation is separately proved for the general state and for the boundary conditions.

Property 1 [$U_n^{b,D} - U_n^{a,D}$ is increasing in n]: In order to prove that

$$U_n^{b,D} - U_n^{a,D} \text{ is increasing in } n \quad (20)$$

Write (20) as follows,

$$\mu_b \delta_b U_{n-1} - \mu_a \delta_a U_{n-1} + \lambda \delta_b U^{b,A}_n - \lambda \delta_a U^{a,A}_n + c_b - c_a \quad (21)$$

Note that (20) is equivalent to $D_n - R_n$. Apply the operators to (21),

$$\begin{aligned} \Theta_n &= \mu_b \delta_b \mathbb{T}U_{n-1} - \mu_a \delta_a \mathbb{T}U_{n-1} + \\ &\lambda \delta_b \mathbb{A}_b U^{b,A}_n - \lambda \delta_a \mathbb{A}_a U^{a,A}_n + c_b - c_a \end{aligned}$$

Divide the proof into two possible cases cases, depending on whether $\mathbb{T}U_{n-1} = \mathbb{T}_b U_{n-1}$ or $\mathbb{T}U_{n-1} = \mathbb{T}_a U_{n-1}$

1) $\mathbb{T}U_{n-1} = \mathbb{T}_b U_{n-1}$. Then,

$$\begin{aligned} \Theta_n &= \mu_b \delta_b (\mu_b \delta_b U_{n-2} + \lambda \delta_b U^{b,A}_{n-1} + c_b) \\ &- \mu_a \delta_a (\mu_b \delta_b U_{n-2} + \lambda \delta_b U^{b,A}_{n-1} + c_b) \\ &+ \lambda \delta_b (\mu_b \delta_b U_n + \lambda \delta_b U^{b,A}_{n+1}) \\ &- \lambda \delta_a (\mu_a \delta_a U_n + \lambda \delta_a U^{a,A}_{n+1}) + c_b - c_a \quad (22) \end{aligned}$$

Write

$$\begin{aligned} \Theta_n &= \mu_b \delta_b (D_{n-2} + c_b) - \mu_a \delta_a (D_{n-2} + c_b) \\ &\lambda \delta_b (D_n) - \lambda \delta_a (R_n) + c_b - c_a \\ &= \mu_b \delta_b (D_{n-2} + c_b) - \mu_a \delta_a (D_{n-2} + c_b) \\ &+ \lambda \delta_b (D_n) - \lambda \delta_a (R_n) + c_b - c_a \\ &- \lambda \delta_a (D_n) + \lambda \delta_a (D_n) \quad (23) \end{aligned}$$

See that D_n and R_n are concave due to the concavity of $U_n^{d,a}$ and $U_n^{r,a}$. Now observe that

$$\mu_b \delta_b - \mu_a \delta_a + \lambda \delta_b - \lambda \delta_a = \gamma \delta_b \delta_a (\mu_b - \mu_a) > 0$$

Use the bound for the slope twice, that is $U_n < U_{n-1} + K$ and $U_n < U_{n+1} + K$ and apply it to D_n . Observe that $\lambda \delta_b - \lambda \delta_a < 0$, and denote $D_n = D_{n-2} + \phi_1(n)$. Hence, $(\lambda \delta_b - \lambda \delta_a) D_n = (D_{n-2} + \phi_1(n))(\lambda \delta_b - \lambda \delta_a)$. Denote $\phi_2(n) = \phi_1(n)(\lambda \delta_a - \lambda \delta_b)$ and write

$$\begin{aligned} \Theta_n &= (\mu_b \delta_b - \mu_a \delta_a + \lambda \delta_b - \lambda \delta_a) D_{n-2} \\ &+ \lambda \delta_a (D_n - R_n) - \phi_2(n) + \kappa, \end{aligned}$$

where $\phi(n)$ is positive decreasing by concavity of $D(n)$ and κ is a suitable constant. Since the expression above is a linear combination of increasing functions with positive coefficients and constants, it is increasing. Hence, the operators do preserve property 1) in this case.

2) $\mathbb{T}U_{n-1} = \mathbb{T}_a U_{n-1}$. The proof is analogous to that of the first case. Similarly to (23) write

$$\begin{aligned} \Theta_n &= \mu_b \delta_b (R_{n-2} + c_a) - \mu_a \delta_a (R_{n-2} + c_a) + \lambda \delta_b (D_n) \\ &- \lambda \delta_a (R_n) + c_b - c_a - \lambda \delta_b (R_n) + \lambda \delta_b (R_n) \end{aligned}$$

Again, use the property of the bounded slope and write

$$\begin{aligned} \Theta_n &= (\mu_b \delta_b - \mu_a \delta_a + \lambda \delta_b - \lambda \delta_a) R_{n-2} \\ &+ \lambda \delta_b (D_n - R_n) - \phi_3(n) + \kappa_1, \end{aligned}$$

where $\phi_3(n)$ is positive decreasing by concavity of $D(n)$ and for some suitable κ_1 . Since the expression above is a linear combination of increasing functions with positive coefficients and constants it is increasing. Hence, the operators preserve property 4) in this case as well.

Property 2 [Concavity]: Apply corresponding operators, $u \in \{a, b\}$:

$$\mathbb{A}_u U_n^{(u,A)} = \mu_u \delta_u U_n + \lambda \delta_u U_{n+1}^{u,A}$$

The result is concave due to the concavity of $U_n, U^{a,A}, U^{b,A}$.

The result for $U^{u,D}$ is similarly deduced.

Apply \mathbb{T} on $U_n - U_{n-1} \geq U_{n+1} - U_n$. We show only non-trivial cases where the threshold is within the range $[n-1, n]$. In the case $n = t$, $D_{t-1} + c_b < R_{t-1} + c_a$

$$D_n - R_{n-1} + c_b - c_a \geq D_{n+1} - R_n + c_b - c_a \geq D_{n+1} - D_n,$$

where the first inequality follows from the fact the sequence $D_{n+1} - R_n$ is decreasing. Apply \mathbb{T} on $U_n - U_{n-1} \geq U_{n+1} - U_n$ in the case $n = t + 1$

$R_n - R_{n-1} > D_n + c_b - c_a - R_{n-1} \geq D_{n+1} + c_b - R_n - c_a$, where the second inequality is due to the fact the sequence $D_{n+1} - R_n$ is decreasing.

Property 3 [Non-decreasing property]: We show that $\mathbb{T}U_n, \mathbb{A}_b U_n^{(b,A)}, \mathbb{A}_a U_n^{(a,A)}$, $n \in \{1, \dots, B\}$ are non-decreasing.

For $\mathbb{T}U_n$, we assume that $U_n \geq U_{n-1}$ and we show that $\mathbb{T}U_n \geq \mathbb{T}U_{n-1}$. Indeed,

$$\mu_b \delta_b U_{n-1} + \lambda \delta_b U_n^{(b,A)} + c_b \geq \mu_b \delta_b U_{n-2} + \lambda \delta_b U_{n-1}^{(b,A)} + c_b$$

For $\mathbb{A}_b U_n^{(b,A)}$ we have,

$$\mu_b \delta_b U_n + \lambda \delta_b U_{n+1}^{(b,A)} \geq \mu_b \delta_b U_n + \lambda \delta_b U_{n+1}^{(b,A)},$$

with equality at B . Similarly, it can be shown that the result holds for \mathbb{A}_a .

Property 4[Slope bound]:

1) $\mathbb{T}U_n - \mathbb{T}U_{n-1} \leq K$,

Note that $\lambda \delta_b + \mu_b \delta_b < 1$. We divide the proof into four cases.

Case 1: $\mathbb{T}U_n = \mathbb{T}_b U_n$ and $\mathbb{T}U_{n-1} = \mathbb{T}_b U_{n-1}$. In this case,

$$\begin{aligned} \mathbb{T}U_n - \mathbb{T}U_{n-1} &\leq \\ &\leq \mu_b \delta_b U_{n-1} + \lambda \delta_b U_n^{b,A} + c_b - \mu_b \delta_b U_{n-2} - \lambda \delta_b U_{n-1}^{b,A} - c_b \\ &\leq \mu_b \delta_b K + \lambda \delta_b K, \\ &\leq K \end{aligned}$$

Hence, the property holds.

Case 2: $\mathbb{T}U_n = \mathbb{T}_a U_n$ and $\mathbb{T}U_{n-1} = \mathbb{T}_a U_{n-1}$. The proof is identical to case 1, and is omitted.

Case 3: $\mathbb{T}U_n = \mathbb{T}_b U_n$ and $\mathbb{T}U_{n-1} = \mathbb{T}_a U_{n-1}$. Write

$$\begin{aligned} \mathbb{T}U_n - \mathbb{T}U_{n-1} &\leq \\ &\mu_b \delta_b U_{n-1} + \lambda \delta_b U_n^{b,A} + c_b - \mu_a \delta_a U_{n-2} - \lambda \delta_a U_{n-1}^{a,A} - c_a \leq \\ &\mu_b \delta_b U_{n-1} + \lambda \delta_b U_n^{b,A} + c_b - \mu_b \delta_b U_{n-2} - \lambda \delta_b U_{n-1}^{b,A} - c_b \leq \\ &\mu_b \delta_b K + \lambda \delta_b K \\ &\leq K \end{aligned}$$

Hence, the property holds.

Case 4: $\mathbb{T}U_n = \mathbb{T}_a U_n$ and $\mathbb{T}U_{n-1} = \mathbb{T}_b U_{n-1}$. This case contradicts property 4 and thus is excluded.

2) $\mathbb{A}_b U_n^{b,A} - \mathbb{A}_b U_{n-1}^{b,A} \leq K$ To show the bound for $U^{b,A}$ write

$$\begin{aligned} \mathbb{A}_b U_n^{b,A} - \mathbb{A}_b U_{n-1}^{b,A} &= \\ &= \delta_b \mu_b U_n + \delta_b \lambda U_{n+1}^{b,A} - \delta_b \mu_b U_{n-1} - \delta_b \lambda U_n^{b,A} \\ &\leq \delta_b (\mu_b + \lambda) K \\ &\leq K \end{aligned}$$

3) $\mathbb{A}_a U_n^{a,A} - \mathbb{A}_a U_{n-1}^{a,A} \leq K$. The proof is identical to the previous one.

4) Boundary conditions

Write boundary conditions for the state B . As $\mathbb{A}_b U_B^{b,A} - \mathbb{A}_b U_{B-1}^{b,A} = 0$, we have

$$\mathbb{A}_b U_B^{b,A} - \mathbb{A}_b U_{B-1}^{d,d} < K$$

The proof for \mathbb{A}_a is similar. The prove for \mathbb{T} at B is similar to that at $n < B$. To see that write:

$$\begin{aligned} \mathbb{T}_b U_B - \mathbb{T}_b U_{B-1} &= \delta_b \mu_b U_{B-1} + \delta_b \lambda U_B^{b,A} - \\ &\delta_b \mu_b U_{B-2} - \delta_b \lambda U_{B-1}^{b,A} \end{aligned}$$

5) Constant K

It is left to select the constant K . We do this by proving the bound for the boundary conditions at 0.

We show that

$$U_1 - U_0 \leq K \Rightarrow \mathbb{T}U_1 - \mathbb{T}U_0 \leq K \quad (24)$$

a) Case 1: Assume $\mathbb{T}U_1 = \mathbb{T}_b U_1$ and $\mathbb{T}U_0 = \mathbb{T}_b U_0$. From (14) we have

$$V_0^{b,D} = \mathbb{T}_b U_0 = \lambda \bar{\delta} V_0^{b,A}$$

Then,

$$\begin{aligned} \mathbb{T}U_1 - \mathbb{T}U_0 &= \\ \mathbb{T}_b U_1 - \mathbb{T}_b U_0 &= \\ \mu_b \delta_b U_0 + \lambda \delta_b U_1^{b,A} + c_b - \lambda \bar{\delta} U_0^{b,A} &= \quad (25) \\ \mu_b \delta_b U_0 - \mu_b \lambda \delta_b \bar{\delta} U_0^{b,A} + c_b + \lambda \delta_b (U_1^{b,A} - U_0^{b,A}) & \quad (26) \end{aligned}$$

$$\leq \mu_b \delta_b U_0 - \mu_b \lambda \delta_b \bar{\delta} U_0^{b,A} + c_b + \lambda \delta_b K$$

(26) is obtained from (25) using the following

$$\begin{aligned} \bar{\delta} - \delta_b &= 1/(\gamma + \lambda) - 1/(\gamma + \lambda + \mu_b) \\ &= (\gamma + \lambda + \mu_b - \gamma - \lambda)/((\gamma + \lambda)(\gamma + \lambda + \mu_b)) \\ &= \mu_b/((\gamma + \lambda)(\gamma + \lambda + \mu_b)) \\ &= \mu_b \delta_b \bar{\delta} \end{aligned}$$

Denote $K_1 = \mu_b \delta_b U_0 - \mu_b \lambda \delta_b \bar{\delta} U_0^{b,A} + c_b$.

b) Case 2: Assume $\mathbb{T}U_1 = \mathbb{T}_a U_1$ and $\mathbb{T}U_0 = \mathbb{T}_a U_0$.

$$V_0^{a,D} = \mathbb{T}_a U_0 = \lambda \bar{\delta} V_0^{a,A}$$

Similarly,

$$\begin{aligned} \mathbb{T}U_1 - \mathbb{T}U_0 &= \\ \mathbb{T}_a U_1^{a,A} - \mathbb{T}_a U_0^{a,A} &= \\ \leq \mu_a \delta_a U_0 - \mu_a \lambda \delta_a \bar{\delta} U_0^{a,A} + c_a + \lambda \delta_a K \end{aligned}$$

Denote $K_2 = \mu_a \delta_a U_0 - \mu_a \lambda \delta_a \bar{\delta} U_0^{a,A} + c_a$.

c) Case 3: Assume $\mathbb{T}U_1 = \mathbb{T}_b U_1$ and $\mathbb{T}U_0 = \mathbb{T}_a U_0$. This case is identical to case 1, because $\mathbb{T}_a U_0 = \mathbb{T}_b U_0$.

K has to satisfy $K_1 + \lambda \delta_b K \leq K$ and $K_2 + \lambda \delta_a K \leq K$, that is, $K_1 \leq (\mu_b + \gamma) \delta_b K$ and $K_2 \leq (\mu_a + \gamma) \delta_a K$. Setting $K = \max \left\{ \frac{K_1}{(\mu_b + \gamma) \delta_b}, \frac{K_2}{(\mu_a + \gamma) \delta_a} \right\}$ suffices to bound the slope in all cases.

This finishes the proof of lemma 1. \square

C. Throughput assessment

In this section we assume that a threshold policy is given. Our aim is to assess the throughput. Recall that given threshold T , the policy consists of transmitting through the most reliable but slowest channel (channel ‘‘a’’, which is, for instance, a relayed channel) if the number of packets in the buffer is smaller than or equal to T at the time at which the transmission starts, and transmitting through the less reliable but fastest channel (channel ‘‘b’’, also known as the direct channel) otherwise. The policy is summarized in Table III. Note that we assume that a packet is removed from the buffer immediately after its transmission ends. Decisions are made immediately after 1) a packet arrives to an empty system, or 2) a packet is removed from the buffer which remains occupied.

TABLE III
TWO CONSIDERED PATHS

channel	reliability	rate	condition for usage (number of buffered packets is)
a	$1 - p_a$, higher	μ_a , lower	smaller than or equal to T
b	$1 - p_b$, lower	μ_b , higher	greater than T

Note that once the SMDP policy is fixed and given, our object of study is a semi-Markov process (SMP). In what follows, we show how to compute the expected impulse reward of the SMP of interest. The resulting metric is the throughput.

Assume that we are given matrix $\mathbf{P}^{(a)}$ (resp., $\mathbf{P}^{(b)}$), whose (i, j) entry indicates the probability that the system contains j packets after a transmission through channel a (resp., b), given that it contained i packets before the transmission. $\mathbf{P}^{(a)}$ and $\mathbf{P}^{(b)}$ are the transition matrices of the embedded chain. Let $P_{ij}^{(a)}$ (resp., $P_{ij}^{(b)}$) be the entry (i, j) of matrix $\mathbf{P}^{(a)}$ (resp., $\mathbf{P}^{(b)}$).

To evaluate the throughput of a threshold policy, with threshold T , we proceed as follows:

- 1) we consider a state space Ω comprising states of the form $\sigma = (i, j)$ where i is the number of packets in the buffer, and j is given as follows,

$$j = \begin{cases} 0 & \text{no packet being transmitted} \\ a & \text{packet being transmitted through channel } a \\ b & \text{packet being transmitted through channel } b \end{cases} \quad (27)$$

Note that the state space comprises states of the form (i, j) such that,

$$(i, j) = \begin{cases} (0, 0) & \text{empty system} \\ (i, a) & 0 < i \leq T \\ (i, b) & T < i \leq B - 1 \end{cases} \quad (28)$$

- 2) Let $|\Omega|$ be the state space cardinality, $|\Omega| = 1 + (B - 1) = B$, where B is the buffer size. Note that if the buffer size is B , we can have at most $B - 1$ packets in the system at any decision epoch. This is because decision epochs occur immediately after departures.
- 3) We build the $|\Omega| \times |\Omega|$ transition matrix \mathbf{P} , corresponding to the given threshold policy.
 - a) if $i = 0$ and $T = 0$, $P_{(i,0),(1,a)} = 1$,
 - b) if $i = 0$ and $T \neq 0$, $P_{(i,0),(1,b)} = 1$,
 - c) if $i > 0$ and $0 < j \leq T$, $P_{(i,a),(j,a)} = P_{ij}^{(a)}$ and $P_{(i,b),(j,a)} = P_{ij}^{(b)}$,
 - d) if $i > 0$ and $j > T$, $P_{(i,a),(j,b)} = P_{ij}^{(a)}$ and $P_{(i,b),(j,b)} = P_{ij}^{(b)}$,
 - e) if $i > 0$ and $j = 0$, $P_{(i,a),(j,0)} = P_{ij}^{(a)}$ and $P_{(i,b),(j,0)} = P_{ij}^{(b)}$.
- 4) We solve $\boldsymbol{\pi} = \boldsymbol{\pi}\mathbf{P}$ to obtain $\boldsymbol{\pi}$, the fraction of visits to each state. The system solution might be obtained using Gaussian elimination (which involves a matrix inversion), or one of its variants, such as GTH [27]. Alternatively, the power method can also be employed.

- 5) We compute the fraction of time at which the system remains at each state, $\tilde{\pi}$. Let τ_σ be the mean time, per visit, at state $\sigma = (i, j)$,

$$\tau_{(i,j)} = \begin{cases} 1/\lambda, & i = 0 \\ 1/\mu_a, & j = a \\ 1/\mu_b, & j = b \end{cases} \quad (29)$$

Then,¹

$$\kappa = \sum_{\forall \sigma \in \Omega} \pi_\sigma \tau_\sigma \quad (30)$$

$$\tilde{\pi}_\sigma = \pi_\sigma \tau_\sigma / \kappa \quad (31)$$

Note that the probability $\sum_{\forall i} \tilde{\pi}_{(i,a)}$ (resp., $\sum_{\forall i} \tilde{\pi}_{(i,b)}$) corresponds to the probability that the system is busy transferring a packet through the channel a (resp., channel b). This follows from the fact that matrix \mathbf{P} characterizes the system dynamics, and its solution yields the system steady state probabilities.

- 6) let ρ_σ be the instantaneous impulse reward (throughput) obtained after a transition from state $\sigma = (i, j)$ to any state σ' ,

$$\rho_{(i,j)} = \begin{cases} 0, & j = 0 \\ 1 - p_a, & j = a \\ 1 - p_b, & j = b \end{cases} \quad (32)$$

- 7) the throughput \tilde{T} is given by

$$\tilde{T} = \sum_{\forall \sigma \in \Omega} \tilde{\pi}_\sigma \rho_\sigma / \tau_\sigma \quad (33)$$

Consider a long interval of time with duration I . The system remains roughly $\tilde{\pi}_\sigma I$ time units at state σ , and visits state σ roughly $\tilde{\pi}_\sigma I / \tau_\sigma$ times. For every visit to state σ , ρ_σ is the obtained impulse reward. Therefore, the expected impulse reward obtained from visits to state σ is $\tilde{\pi}_\sigma \rho_\sigma I / \tau_\sigma$. Normalizing by the duration I , we obtain the expected impulse reward per time unit derived from state σ , which is $\tilde{\pi}_\sigma \rho_\sigma / \tau_\sigma$. Summing for all states, we obtain the system throughput.

Equivalently,

$$\tilde{T} = \left(\sum_{\forall i} \tilde{\pi}_{(i,a)} \right) \mu_a (1 - p_a) + \left(\sum_{\forall i} \tilde{\pi}_{(i,b)} \right) \mu_b (1 - p_b) \quad (34)$$

Special cases:

- **Exponential service times:** in case the service times are exponentially distributed, policy evaluation consists of computing the expected instantaneous reward of a continuous-time Markov chain. In this case, tools like Tangram-II [26] can be used to compute the metrics of interest. The system can be solved either using the embedded process (as described in this section – see Figure 10), or directly using the natural process (see Figure 11).
- **Deterministic service times:** special solution methods can be used to efficiently compute the throughput if service times are deterministic. In particular, Tangram-II implements the methods proposed in [24] for this purpose.

¹The rationale is given, for instance, in http://www.cs.toronto.edu/~marbach/COURSES/CSC2206_F14/semi_markov.pdf.

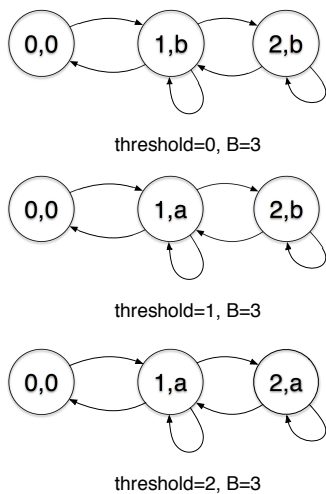


Fig. 10. Policy evaluation using the embedded process. The discrete time Markov chains of the embedded process, as illustrated in this figure, are applicable for the assessment of the throughput given generally distributed service times.

Alternatively, the equations for the embedded Markov chain follow from the discussion in Section III-B and can be used to assess the throughput using the ideas presented in this appendix.

- **Uniform service times:** the equations for the embedded Markov chain have been presented in Section III-C. Together with the algorithm introduced in this appendix, the throughput can be assessed.
- **Other service time distributions:** to compute the throughput under other service time distributions, one can rely on tools such as Oris [25]. Table IV illustrates the input to Oris. The input comprises three state variables, W, S_a, S_b , characterizing the number of waiting packets, and the number of packets being transmitted through channels a and b , respectively. Note that $W \in \{0, 1, \dots, B-1\}$, $S_a \in \{0, 1\}$ and $S_b \in \{0, 1\}$.

The discrete time Markov chains illustrated in Figure 10 correspond to the process embedded at instants of (i) service completions and (ii) arrivals to an empty system, as described in Section III. Note that these Markov chains model generally distributed service times. This is in contrast to the discrete time Markov chains subsumed by the MDP presented in Figure 2, which is applicable to exponentially distributed service times. In the MDP model presented in Figure 2 the embedded points consist of all departures and arrivals.

In the particular case of exponentially distributed service times, the throughput can also be assessed directly using the natural continuous time process, which is illustrated in Figure 11. In this section we focused on the use of the embedded process. A further discussion of the different approaches is presented in [16].

REFERENCES

- [1] D. Tse and P. Viswanath, *Fundamentals of wireless communication*. Cambridge university press, 2005.
- [2] L. Zheng and D. N. Tse, "Diversity and multiplexing: a fundamental tradeoff in multiple-antenna channels," *Trans. Info. Theory*, 2003.

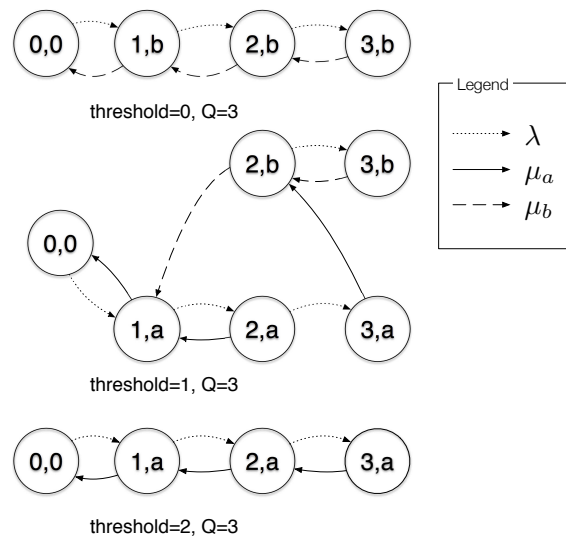


Fig. 11. Policy evaluation using the natural process. The continuous time Markov chains of the natural process, as illustrated in this figure, are applicable for the assessment of the throughput when service times are exponentially distributed.

TABLE IV
THRESHOLD POLICY CHARACTERIZATION

event	inter-event time	condition	update
packet arrival	exponential, rate λ	$W + S_a + S_b < B$	$W \leftarrow W + 1$
service start			
service a	0 (instantaneous)	$W > 0$ and $S_a = 0$ and $S_b = 0$ and $W \leq T$	$W \leftarrow W - 1,$ $S_a \leftarrow S_a + 1$
service b	0 (instantaneous)	$W > 0$ and $S_a = 0$ and $S_b = 0$ and $W > T$	$W \leftarrow W - 1,$ $S_b \leftarrow S_b + 1$
service completion			
service a	general, rate μ_a	$S_a = 1$	$S_a \leftarrow S_a - 1$
service b	general, rate μ_b	$S_b = 1$	$S_b \leftarrow S_b - 1$

- [3] S. Karmakar and M. K. Varanasi, "The diversity-multiplexing tradeoff of the dynamic decode-and-forward protocol on a mimo half-duplex relay channel," *Trans. Info. Theory*, vol. 57, no. 10, 2011.
- [4] J. N. Laneman, D. N. Tse, and G. W. Wornell, "Cooperative diversity in wireless networks: Efficient protocols and outage behavior," *Info. Theory, IEEE Trans. on*, vol. 50, no. 12, pp. 3062-3080, 2004.
- [5] R. Heath and A. Paulraj, "Diversity versus multiplexing in narrowband mimo channels," *submitted Dec*, 2002.
- [6] D. N. C. Tse, P. Viswanath, and L. Zheng, "Diversity-multiplexing tradeoff in multiple-access channels," *Signal. Info. Theory*, 2004.
- [7] Y.-C. Liang, K.-C. Chen, G. Y. Li, and P. Mahonen, "Cognitive radio networking and communications," *Trans. Vehic. Techn.*, 2011.
- [8] R. Berry and R. Gallager, "Communication over fading channels with delay constraints," *Trans. Info. Theory*, 2002.
- [9] B. E. Collins and R. L. Cruz, "Transmission policies for time varying channels with average delay constraints," in *Allerton*, 1999.
- [10] A. Scaglione, D. L. Goeckel, and J. N. Laneman, "Cooperative communications in mobile ad hoc networks," *Signal Proc. Mag.*, 2006.
- [11] L. Tassiulas and A. Ephremides, "Stability properties of constrained queueing systems and scheduling policies for maximum throughput in multihop radio networks," *Automatic Control, Trans.*, vol. 37, no. 12, pp. 1936-1948, 1992.
- [12] E. M. Yeh and R. A. Berry, "Throughput optimal control of cooperative relay networks," *Info. Theory, Trans.*, 2007.
- [13] S. Supittayapornpong and M. J. Neely, "Achieving utility-delay-reliability tradeoff in stochastic network optimization with finite buffers," *arXiv preprint arXiv:1501.03457*, 2015.
- [14] R. Urgaonkar and M. J. Neely, "Delay-limited cooperative communication w/reliability constraints in wireless networks," *Trans. Info. Theory*, 2014.

- [15] E. Altman, K. Avrachenkov, N. Bonneau, M. Debbah, R. El-Azouzi, and D. S. Menasché, “Constrained stochastic games in wireless networks,” in *Globecom*. IEEE, 2007, pp. 315–320.
- [16] M. L. Puterman, *Markov Decision Processes: Discrete Stochastic Dynamic Programming*. John Wiley & Sons, Inc., 1994.
- [17] G. Koole, “Structural results for the control of queueing systems using event-based dynamic programming,” *Queueing Systems*, 1998.
- [18] B. Hajek, “Optimal control of two interacting service stations,” *IEEE Transactions on Automatic Control*, vol. 29, no. 6, pp. 491–499, 1984.
- [19] L. I. Sennott, *Stochastic dynamic programming and the control of queueing systems*. John Wiley & Sons, 2009, vol. 504.
- [20] J. Walrand, *An introduction to queueing networks*. Prentice Hall, 1988.
- [21] D. S. Menasché, D. Goeckel, and D. Towsley, “Optimal forwarding strategies for the relay channel under average delay constraints,” in *ACM Wireless S3*, 2010, pp. 1–4.
- [22] D. Bertsekas, *Dynamic programming and optimal control*. Athena Scientific Belmont, MA, 1995, vol. 2, no. 2.
- [23] M. Reed and B. Simon, *Methods of modern mathematical physics: Functional analysis*. Gulf Professional Publishing, 1980, vol. 1.
- [24] E. de Souza e Silva, H. R. Gail, and R. R. Muntz, *Efficient solutions for a class of non-Markovian models*. Springer, 1995.
- [25] P. Ballarini, N. Bertrand, A. Horváth, M. Paolieri, and E. Vicario, “Transient analysis of networks of stochastic timed automata using stochastic state classes,” in *Quantitative Evaluation of Systems*. Springer, 2013, pp. 355–371.
- [26] E. de Souza e Silva and R. M. Leao, “The Tangram-II environment,” in *Computer Performance Evaluation. Modelling Techniques and Tools*. Springer, 2000, pp. 366–369.
- [27] W. K. Grassmann, M. I. Taksar, and D. P. Heyman, “Regenerative analysis and steady state distributions for markov chains,” *Operations Research*, vol. 33, no. 5, pp. 1107–1116, 1985.